Coherent Optical polarization of Bulk GaAs Studied by Femtosecond Photon-Echo Spectroscopy

Coherent Optical Polarization of Bulk GaAs Studied by Femtosecond Photon-Echo Spectroscopy

A. Lohner, K. Rick, P. Leisching, A. Leitenstorfer, and T. Elsaesser*
Physik Department E 11, Technische Universität München, D-8046 Garching, Germany

T. Kuhn
Institut für Theoretische Physik, Universität Stuttgart, D-7000 Stuttgart 80, Germany

F. Rossi
Dipartimento di Fisica, Università di Modena, 1-41100 Modena, Italy

W. Stolz
Zentrum für Materialwissenschaften, Universität Marburg, D-3550 Marburg, Germany
(Received 8 March 1993)

The nonlinear polarization close to the band gap of GaAs is studied by spectrally and temporally resolved four-wave mixing. Excitonic and free carrier contributions both excited within the bandwidth of the 100 fs pulses are distinguished for the first time. The excitonic part dominates at carrier densities below 10^{16} cm^{-3}. At higher density, nonthermalized free carriers give rise to an additional component resonant to the pulse that shows a photon-echo-like time behavior. Monte Carlo simulations including the coherent polarization and the scattering dynamics of the carriers account for the data.

PACS numbers: 42.65.Re, 71.35.+z, 78.47.+p

Direct-gap semiconductors exhibit large third-order optical nonlinearities in the range of the fundamental band gap that are caused by excitons and/or free electron-hole pairs. Excitation with coherent light results in a phase coherent nonlinear polarization which decays subsequently by phase-breaking scattering processes of the photoexcited carriers, occurring on a subpicosecond time scale. The nonlinear polarization gives insight into the interaction among photoexcited carriers and their nonequilibrium dynamics which have been studied by transient coherent spectroscopy using ultrashort laser pulses [1–10].

The excitonic polarization in bulk GaAs has been investigated by degenerate four-wave mixing (FWM) in the picosecond regime [6]. At carrier densities below 10^{14} cm^{-3}, dephasing times as long as $T_2=7$ ps have been measured, whereas a faster loss of phase coherence by exciton-exciton collisions was observed at higher excitation levels of several 10^{15} cm^{-3}. Additional generation of free electron-hole pairs leads to an even stronger shortening of T_2 down to $T_2<1$ ps which is due to exciton-free carrier collisions.

Dephasing of electron-hole excitations has been studied with femtosecond pulses both around the band gap $E_G \simeq 1.5$ eV and at 2 eV [7–9]. For excitation with 500 fs pulses below the threshold of LO phonon emission, values of $T_2 \simeq 300$ fs have been derived from hole burning measurements with an excitation density of 5×10^{17} cm^{-3} [7]. The rapid loss of phase coherence was attributed to collisions among free carriers. In contrast, much shorter T_2 times between 20 and 60 fs for carrier densities from 8×10^{17} to 10^{17} cm^{-3} were extracted from measurements with pulses of 6 to 10 fs duration [8,9].

In many femtosecond experiments (e.g., [8]), the large spectral width of the pulses results in excitation of both excitonic and free carrier states, an effect that has been completely neglected in the analysis of previous data. The two types of excitations and their interaction via many-body effects should lead to significant changes of the overall third-order polarization compared to cases of selective excitation. For instance, the time evolution of excitonic contributions should show features of a free induction decay whereas free carrier states should exhibit a photon echo [10]. In this Letter, we present the first femtosecond study giving direct insight into the fundamental properties of third-order nonlinearities due to simultaneously excited excitons and free carriers in bulk GaAs. We demonstrate that the spectrally resolved signal in FWM experiments with 100 fs pulses provided new information on the nature of coherent polarizations. The excitonic polarization dominates at carrier densities below 10^{16} cm^{-3}, whereas an additional component due to nonthermalized free carriers is found at higher densities. The temporally resolved FWM signal gives a different time behavior of the two contributions.

A 0.5 μm thick GaAs layer clad by AlGaAs barriers [11] was studied in the FWM experiment depicted schematically in Fig. 1(a). The 100 fs pulses 1 and 2 of identical wavelength generate a transient grating in the sample from which a FWM signal is emitted by self-diffraction into the direction $\mathbf{k}_d=2\mathbf{k}_2-\mathbf{k}_1$. This signal is studied by the following techniques: (i) The spectrally and temporally integrated intensity is recorded as a function of the delay time T_{12} between the pulses 1 and 2; (ii) the FWM signal is spectrally dispersed with the help of a monochromator (resolution 2 meV); (iii) the temporal envelope is measured by convoluting the signal with a third laser pulse via sum-frequency mixing in a nonlinear

0031-9007/93/71(1)/77(4)$06.00

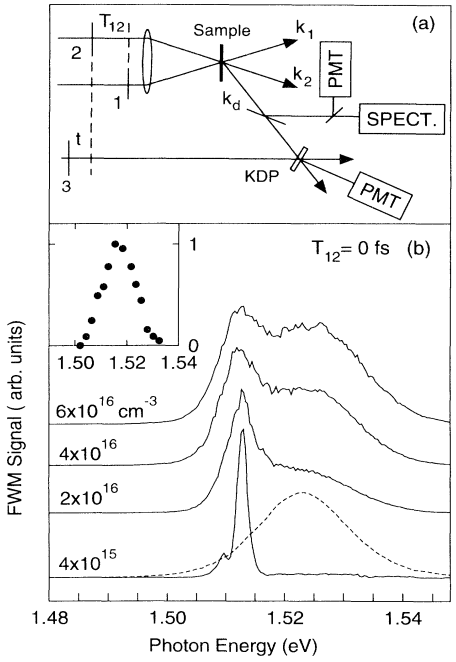

FIG. 1. (a) Schematic of the degenerate FWM experiment. The pulses 1 and 2 create a transient grating in the sample giving rise to a signal that is spectrally and temporally analyzed (SPECT, monochromator; PMT, photomultipliers). (b) Spectrally resolved FWM signal at delay zero ($T_{12}=0$) after excitation with pulses centered at 1.523 eV (dashed line: spectrum of the pulses). The diffracted intensity is plotted for excitation densities from 4×10^{15} to 6×10^{16} cm^{-3}. Inset: Spectrally integrated intensity of the FWM signal at $T_{12}=0$ as a function of the (peak) photon energy of the pulses.

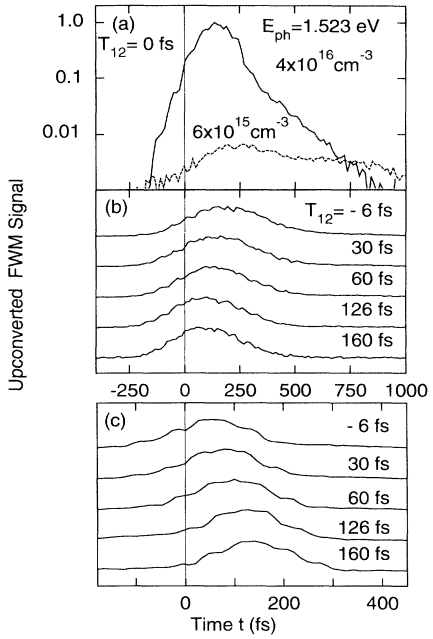

FIG. 2. Temporal profiles of the FWM signal. The intensity is plotted vs the delay time t between pulses 2 and 3 for different delays T_{12} between pulse 1 and pulse 2 [cf. Fig. 1(a)]. (a) Time envelope of the spectrally integrated FWM signal measured with carrier densities N_{ex} of 6×10^{15} cm^{-3} and 4×10^{16} cm^{-3} ($T_{12}=0$, logarithmic ordinate). (b) Excitonic component signal after spectral selection ($N_{ex}=4\times10^{16}$ cm^{-3}, linear ordinate scale). (c) Free carrier signal after spectral selection. The data for different T_{12} show a photon echo. Note the different time scales of (a), (b), and (c).

KDP crystal (thickness 0.5 mm, type-II phase matching). Transform-limited pulses of 100 fs duration (spectral width 20 meV) are generated with a mode-locked Ti:sapphire laser. The excitation densities given below are estimated from the absorption of the sample and the incident flux of laser photons.

First, we study the *spectrally* and *temporally integrated* FWM signal. In the inset of Fig. 1(b), the normalized intensity at delay zero ($T_{12}=0$) is plotted versus the spectral position of the laser pulses for an excitation density of 4×10^{15} cm^{-3}. We find a strong resonant enhancement at the exciton absorption line ($E\simeq1.513$ eV). The width of this profile is determined by the bandwidth of the laser pulses of 20 meV. For increasing delay time T_{12}, the signal follows a monoexponential decay. The decay times are $\tau\simeq110$ fs for excitation at or below 1.513 eV and less than 70 fs at higher photon energies.

More specific information on the origin of the third-order polarization is gained from *spectrally resolved* FWM signals which are plotted in Fig. 1(b) (solid lines) for four different excitation densities N_{ex}. The dashed line gives the spectral profile of the excitation pulses centered at 1.523 eV in the free carrier continuum. For $N_{ex}\leq10^{16}$ cm^{-3}, we observe a strong excitonic component at 1.513 eV with a spectral width of less than $\frac{1}{5}$ of the laser bandwidth. With increasing N_{ex}, this line broadens and a second contribution occurs around the maximum of the laser spectrum.

The two components of the nonlinear polarization show a different time behavior. In Fig. 2(a), the up-converted overall intensity diffracted from the grating for $T_{12}=0$ is plotted versus the delay time t between pulse 3 and pulse 2 [cf. Fig. 1(a)]. The excitonic polarization at low density shows a delayed rise and a decay on a time scale of 1 ps. At higher density, the decay is faster and superimposed at early times by the short pulse-limited signal due to free carriers. For an isolated observation of the two components, the free carrier *or* the excitonic signal selected by interference filters was convoluted with pulse 3 [12]. The temporal envelope of the excitonic signal in Fig. 2(b) shows only slight changes with delay time T_{12}. A similar behavior is found at low excitation densities. In contrast, the peak of the free carrier contribution [Fig. 2(c)] for increasing delay times T_{12} moves linearly to positive values of t, a clear indication of a photon echo.

In our experiments, the bandwidth of the 100 fs pulses of 20 meV is substantially larger than the excitonic bind-

ing energy of 4.2 meV. Exciton *and* free carrier states are excited simultaneously and both contribute to the overall optical nonlinearity as is directly evident from the spectrally resolved FWM signals [Fig. 1(b)]. The very strong excitonic enhancement at low carrier densities is due (i) to the large ratio $d_{ex}/d_{con} \simeq 10$ of the excitonic (d_{ex}) and the interband (d_{con}) oscillator strength [13,14] and (ii) to the slow dephasing of the excitonic polarization which persists much longer than the free carrier signal [cf. Fig. 2(a)]. For densities above 10^{16} cm^{-3}, excitonic and free carrier contributions are of similar strength. With increasing concentration of free carriers, screening of the attractive electron-hole (e-h) interaction lowers the ionization continuum of excitons, leading to a decrease of the excitonic oscillator strength and of the resonant enhancement.

The time-resolved data of Fig. 2 demonstrate the distinctly different temporal behavior of the two parts of the nonlinear polarization. The free carrier states optically coupled by the femtosecond pulses represent an inhomogeneously broadened ensemble giving rise to a photon echo [Fig. 2(c)]. The loss of phase coherence by carrier-carrier collisions results in a decay time which is shorter than our time resolution of 70 fs. For an excitation density of 4×10^{16} cm^{-3}, a reduction of the scattering rates by Pauli blocking of electronic states [15] is negligible in our nonequilibrium situation. In contrast, the experiments of Ref. [7] giving T_2 times around 300 fs were performed at much higher densities where those effects might be important. The time envelope of the excitonic FWM signal is strongly influenced by many-body effects [4,5,10]. Recent studies of excitons in GaAs/AlGaAs quantum wells showed a prompt signal emitted immediately after pulse 2, and a stronger delayed component with a maximum around $t = T_2$ [5]. In our case, the short dephasing times are close to the pulse duration and, consequently, prompt and delayed contributions give rise to a time envelope with a single broad maximum at a time t that depends only weakly on T_{12}.

For a quantitative analysis of our data, a recently proposed technique for the solution of the semiconductor Bloch equations [16] has been generalized to account for the FWM geometry. Four Fourier components of the polarization ($\mathbf{k}_1$, $\mathbf{k}_2$, $2\mathbf{k}_2-\mathbf{k}_1$, $2\mathbf{k}_1-\mathbf{k}_2$) and three components of the distribution functions ($\mathbf{k}=0$, $\mathbf{k}_1-\mathbf{k}_2$, $\mathbf{k}_2-\mathbf{k}_1$) are included [10]. A Monte Carlo simulation for the distribution functions including carrier-carrier and carrier-phonon scattering is combined with a direct integration technique for the polarizations [17]. The dephasing contribution due to carrier-carrier scattering is modeled by a constant rate. Details of the numerical method are given in Ref. [16].

The calculated spectra of the FWM signal are shown in Fig. 3(a). As observed in the experiment [Fig. 1(b)], the signal is concentrated at the exciton energy up to a density of 10^{16} cm^{-3}. A free carrier contribution centered at the incident pulses appears above 10^{16} cm^{-3} and increases with density. The overall agreement between theory and experiment is very good. There are, however, some slight differences: In the calculated spectra, the exciton line exhibits a redshift with increasing density and the free carrier contribution begins to dominate at lower densities than in the experiments. We attribute this difference to limitations of the static screening model used in the calculations. Even at equilibrium it has been found that the dielectric function within the single-plasmon pole approximation overestimates the screening [14]. Better agreement has been obtained by using a fit parameter $C=4$ [see Eq. (6) in Ref. [10]] which increases the plasmon contribution in the screened Coulomb potential. This value has also been used in our calculations. Under the ultrafast excitation conditions of the present experiments, dynamical aspects of the screening are expected to become even more important [18,19]. A full modeling would require a screened Coulomb potential depending explicitly on two times t_1 and t_2 to account correctly for the buildup of screening. However, up to now there exist only preliminary investigations of this effect [20,21], which do not include a full numerical solu-

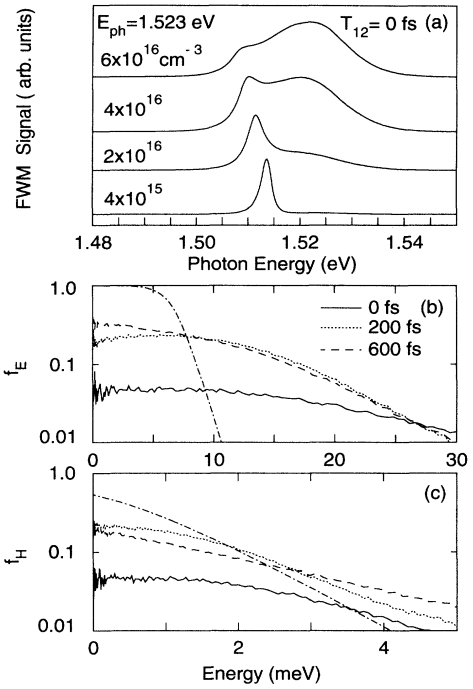

FIG. 3. Results of the Monte Carlo simulations. (a) Spectra of the FWM signal for the parameters of the femtosecond experiments [cf. Fig. 1(b)]. (b) and (c) Electron (f_E) and hole (f_H) distribution functions for different times t after formation of the transient grating ($T_{12}=0$, carrier density 4×10^{16} cm^{-3}) as a function of the carrier kinetic energy. The dash-dotted lines represent equilibrium distributions for a temperature of 10 K.

tion of the semiconductor Bloch equations. The interpretation given above is supported by a simulation where the screening is reduced further ($C=20$) and indeed a smaller redshift and stronger exciton lines in the spectrum are found.

Theoretical and experimental studies of the absorption spectra of bulk GaAs give a (Mott) density $N_c \simeq 4\times10^{15}$ cm^{-3} of thermalized free carriers at a temperature of 10 K for which the exciton ground state merges into the continuum [13,14]. Our FWM spectra, however, show excitonic signals up to $N_{ex} \simeq 6\times10^{16}$ cm^{-3}, much higher than N_c. This behavior is caused by the broad, initially nonthermal distributions of electrons and holes which screen the attractive e-h interaction less effectively. In Figs. 3(b) and 3(c), calculated distribution functions are plotted for different times t during and after excitation ($T_{12}=0$). The dominant energy exchange process on these short time scales is electron-hole scattering which leads to cooling of electrons and heating of holes. From the exponential tails, we estimate an electron temperature of 80 K and a hole temperature of 30 K for $t > 200$ fs. The elevated temperatures lead to an increase of the excitonic Mott density compared to screening of cold carrier distributions (dash-dotted line).

In conclusion, the results presented here give the first direct insight into third-order optical polarizations occurring close to the band gap of bulk GaAs after simultaneous excitation of excitons and free carriers. Femtosecond four-wave-mixing studies and their analysis by Monte Carlo simulations reveal an excitonic nonlinearity which dominates at carrier densities below 10^{16} cm^{-3} and shows a dynamics governed by many-body effects. For stronger excitation, hot free carriers reduce the excitonic contribution via screening and give rise to an additional component with photon-echo-like time behavior.

*Present address: Max-Born-Institut für Nichtlineare Optik und Kurzzeitspektroskopie, Rudower Chaussee 6, O-1199 Berlin, Germany.

[1] K. Leo, M. Wegener, J. Shah, D. S. Chemla, E. O. Göbel, T. C. Damen, S. Schmitt-Rink, and W. Schäfer, Phys. Rev. Lett. **65**, 1340 (1990).
[2] M. Wegener, D. S. Chemla, S. Schmitt-Rink, and W. Schäfer, Phys. Rev. A **42**, 5675 (1990).
[3] M. D. Webb, S. T. Cundiff, and D. G. Steel, Phys. Rev. Lett. **66**, 934 (1991).
[4] S. Weiss, M.-A. Mycek, J.-Y. Bigot, S. Schmitt-Rink, and D. S. Chemla, Phys. Rev. Lett. **69**, 2685 (1992).
[5] D. S. Kim, J. Shah, T. C. Damen, W. Schäfer, F. Jahnke, S. Schmitt-Rink, and K. Köhler, Phys. Rev. Lett. **69**, 2725 (1992).
[6] L. Schultheis, J. Kuhl, A. Honold, and C. W. Tu, Phys. Rev. Lett. **57**, 1635 (1986); **57**, 1797 (1986).
[7] J. L. Oudar, D. Hulin, A. Migus, A. Antonetti, and F. Alexandre, Phys. Rev. Lett. **55**, 2074 (1985).
[8] M. T. Portella, J.-Y. Bigot, R. W. Schoenlein, J. E. Cunningham, and C. V. Shank, Appl. Phys. Lett. **60**, 2123 (1992).
[9] P. C. Becker, H. L. Fragnito, C. H. BritoCruz, R. L. Fork, J. E. Cunningham, J. E. Henry, and C. V. Shank, Phys. Rev. Lett. **61**, 1647 (1988).
[10] M. Lindberg, R. Binder, and S. W. Koch, Phys. Rev. A **45**, 1865 (1992).
[11] The GaAs substrate was removed by selective etching to allow for transmission measurements.
[12] Spectral filtering results in a temporal broadening of the signal of less than 50 fs, i.e., short compared to the pulse duration.
[13] R. G. Ulbrich, in *Optical Nonlinearities and Instabilities in Semiconductors,* edited by H. Haug (Academic, New York, 1988), p. 121.
[14] H. Haug and S. Schmitt-Rink, Prog. Quantum Electron. **9**, 3 (1984).
[15] D. S. Kim, J. Shah, J. E. Cunningham, T. C. Damen, and W. Schäfer, Phys. Rev. Lett. **68**, 2838 (1992).
[16] T. Kuhn and F. Rossi, Phys. Rev. Lett. **69**, 977 (1992); Phys. Rev. B **46**, 7496 (1992).
[17] In the calculations, a finite pulse duration of 100 fs is taken into account.
[18] T. Elsaesser, J. Shah, L. Rota, and P. Lugli, Phys. Rev. Lett. **66**, 1757 (1991).
[19] D. C. Scott, R. Binder, and S. W. Koch, Phys. Rev. Lett. **69**, 347 (1992).
[20] M. Hartmann, H. Stolz, and R. Zimmermann, Phys. Status Solidi (b) **159**, 35 (1989).
[21] H. Haug and C. Ell, Phys. Rev. B **46**, 2126 (1992).